Published in final edited form as:
Free Radic Biol Med. 2014 July ; 72: 296–307. doi:10.1016/j.freeradbiomed.2014.04.004.

AKT/mTOR and C-Jun N-terminal Kinase (JNK) Signaling Pathways Are Required for Chrysotile Asbestos-Induced Autophagy

Ziying Lin[a,1], **Tie Liu**[b,1], **David W Kamp**[c,*], **Yahong Wang**[a], **Huijuan He**[a], **Xu Zhou**[a], **Donghong Li**[a], **Lawei Yang**[a], **Bin Zhao**[a], and **Gang Liu**[a,*]

[a]Clinical Research Center, Affiliated Hospital of Guangdong Medical College, Zhanjiang, 524001, China

[b]Department of Hematology, The Second Affiliated Hospital, Medical School of Xi'an Jiaotong University, Xi'an 710004, Shanxi, China

[c]Department of Medicine, Northwestern University Feinberg School of Medicine and Jesse Brown VA Medical Center, 240 E. Huron, McGaw M-330, Chicago, IL 60611, USA

Abstract

Chrysotile asbestos is closely associated with excess mortality from pulmonary diseases such as lung cancer, mesothelioma, and asbestosis. Although multiple mechanisms in which chrysotile asbestos fibers induce pulmonary disease have been identified, the role of autophagy in human lung epithelial cells has not been examined. In the present study, we evaluated whether chrysotile asbestos induces autophagy in A549 human lung epithelial cells, and then analyzed the possible underlying molecular mechanism. Chrysotile asbestos-induced autophagy in A549 cells based on a series of biochemical and microscopic autophagy markers. We observed that asbestos increased A549 cell microtubule-associated protein 2 light chains 3 (LC3-II) expression, an autophagy marker, in conjunction with dephosphorylation of phospho-AKT, phospho-mTOR, and phospho-P70s6k. Notably, AKT1/AKT2 double knockout (AKT DKO) murine embryonic fibroblasts (MEFs) had negligible asbestos-induced LC3-II expression supporting a crucial role for AKT signaling. Chrysotile asbestos also led to the phosphorylation/activation of Jun N-terminal kinase (JNK) and p38 MAPK. Pharmacologic inhibition of JNK, but not p38 MAPK, dramatically inhibited the protein expression of LC3-II. Moreover, $JNK2^{-/-}$ MEFs but not $JNK1^{-/-}$ MEFs blocked LC3-II levels induced by chrysotile asbestos. In addition, NAC, an antioxidant, attenuated chrysotile asbestos-induced dephosphorylation of p-AKT and completely abolished phosphorylation/activation of JNK. Finally, we demonstrated that chrysotile asbestos-induced

Address for correspondence: *Gang Liu, M.D. Ph.D. Clinical Research Center, Affiliated Hospital of Guangdong Medical College, Zhanjiang, 524001, China; Fax: +86-0759-2369561, gangliu11@gdmc.edu.cn. *David W. Kamp, M.D. Northwestern University Feinberg School of Medicine, Pulmonary and Critical Care Medicine, McGaw M-330, 240 E. Huron St., Chicago, IL 60611-3010. d-kamp@northwestern.edu.

[1]Z.Y.-L and T.-L contributed equally as first authors.

apoptosis was not affected by the presence of the autophagy inhibitors 3-methyladenine (3-MA) or ATG5 (autophagy-related gene 5) siRNA, indicating that chrysotile asbestos-induced autophagy may be adaptive rather than prosurvival. Our findings demonstrate that AKT/mTOR and JNK2 signaling pathways are required for chrysotile asbestos-induced autophagy. These data provide a mechanistic basis for possible future clinical applications targeting these signaling pathways in the management of asbestos-induced lung disease.

Keywords

chrysotile asbestos; autophagy; LC3-II; pulmonary disease; A549 cells

Introduction

Environmental or occupational exposure to asbestos fibers (e.g. chrysotile or amphiboles such as crocidolite, amosite, and others) increase the risk for chronic respiratory diseases, including interstitial lung fibrosis (e.g. asbestosis), lung cancer, and pleural malignant mesothelioma (MM) [1, 2]. The mechanisms of injury to cells of the lung and pleura that results in lung diseases following asbestos exposure are not fully established [1, 3, 4]. All forms of asbestos, including chrysotile, are carcinogens that can promote iron-derived free radical formation *in vitro*, injure lung target cells, and induce asbestosis, lung cancer, and mesothelioma in human [4, 5]. Asbestos fibers activate epidermal growth factor receptor (EGFR) and other receptors leading to activation of the mitogen-activated protein kinase (MAPK) pathway including p38, c-Jun N-terminal kinase (JNK) and extracellular signal regulated kinase(ERK1/2) as well as AKT that can modulate apoptosis [6, 7].

Autophagy is a highly conserved homeostatic pathway in eukaryotic cells involved in multiple physiologic and pathophysiologic functions involving clearance of misfolded or aggregated proteins, providing alternative metabolic fuel sources, clearing damaged organelles (e.g. mitochondria), eliminating intracellular pathogens, and regulating cell death [8, 9]. Autophagy also affects varied immune system functions such as antigen presentation, lymphocyte development, inflammasome formation and cytokine secretion [10–12]. Autophagy can be adaptive; pro-survival in certain settings while in other settings is implicated in aging as well as malignant or degenerative disease pathogenesis. In the lungs, autophagy-dependent mechanisms have been implicated in diverse pulmonary diseases including pulmonary fibrosis, chronic obstructive pulmonary disease, cystic fibrosis and pulmonary hypertension [8, 9, 13, 14]. Precisely how autophagy mediates these various diseases is an area of ongoing investigation. Autophagy modulates the apoptotic pathway at the signal transduction level impacting the decision of a cell to undergo programmed cell death [15]. Recent studies have demonstrated that PI3K/AKT/mTOR signaling pathways play a crucial role in regulating autophagy. However, the function of autophagy in human diseases as well as the crosstalk between autophagy and MAPK signaling is uncertain.

Reactive oxygen species (ROS) have been identified as signaling molecules important in various pathways, including autophagy [16,17]. Accumulating evidence show a key role for

ROS in asbestos-induced toxicity and lung disease [18]. However, the role of ROS in modulating signaling proteins involved in asbestos-induced autophagy is not established.

Lung epithelial cells are important target cells of asbestos fibers. As reviewed elsewhere [4], work by others as well as our group have shown that asbestos-induced pulmonary toxicity is mediated in part by lung epithelial cell mitochondrial dysfunction, mitochondrial reactive oxygen species (ROS) production, DNA damage, p53 activation and mitochondria-regulated apoptosis. However, the role of autophagy in modulating asbestos-induced lung epithelial cell toxicity is unknown. Our previous studies focused on the effects of amosite asbestos on lung epithelial cells [2, 4, 19, 20]. In the present study, we demonstate that chrysotile asbestos induces autophagy in human lung epithelial cell (A549) using ultrastructural and biochemical features that are associated with autophagy. This investigation also presents evidence demonstrating that chrysotile-induced autophagy is associated with altered signaling via the AKT/mTOR and JNK2 pathways in human lung epithelial cells.

Materials and methods

Materials

Dulbecco's modified Eagle's medium (DMEM) culture mediate, penicillin, streptomycin and fetal bovine serum (FBS) were purchased from Invitrogen-Life Technologies (Carlsbad, CA). Acridine orange (AO) (235474), monodansylcadaverine (MDC) (30432), rapamycin (R0395), trypsin-EDTA, N-acetyl cysteine (NAC) (A7250), 3-methyladenine (3-MA) (M9281) were obtained from Sigma-Aldrich (St. Louis, MO). E64d (330005), Pepstatin A1 (516483), SB203580, pifithrin-α (PFT-α) were purchased from Calbiochem (Merk KGaA, Darmstadt, Germany). AKT(9272), phospho-AKT(4060, Ser473), mTOR(2972), phospho-mTOR(5536), p70S6K(9202), phospho-p70S6K(9234), LC3A/B(4108), p38(9212), phospho-p38(4511), ERK1/2(4695), phospho-ERK(4377), JNK(9258), phospho-JNK(4668), phospho-p53(9284), SP600125 (9901), and actin(4790)antibodies were obtained from Cell Signaling Technology (Beverly, MA). Amplex® Red Reagent (A12222), Hydroethidin(D23107), Lipofectamine 2000 and TRIzol reagent were from Invitrogen Life Technologies (Carlsbad, CA). pBABE-EGFP-mCherry-LC3 was purchased from Biovector Science Lab, Inc (China). ATG5 siRNA was purchased from Suzhou GenePharma Co., Ltd, China.

Pretreatment of chrysotile asbestos

Chrysotile asbestos fibers used in these experiments were mined from Qinghai, China. We used the International Union Against Cancer standard reference for chrysotile asbestos (average length, 7.8 μm; average diameter, 0.2 μm) in these studies [21]. The fibers were prepared as described previously [22]. Briefly, samples of fibers were weighed and crushed into ultrafine powder by a crusher. After ultra-sonication for 10 min, the mixtures were centrifuged at 2000 rpm for 10 min, the supernatants were removed and the pellets were washed with 2 ml distilled water. Each chrysotile asbestos was then re-suspended in PBS for the cell treatment. A stock solution of the fibers (5 mg/mL) was sterilized by autoclaving and mixed to ensure a uniform suspension before being diluted with tissue culture medium for cell treatment.

Cell culture and treatment

Human lung carcinoma A549 cell was purchased from American Tissue Culture Collection (ATCC) (Rockville, MD, USA). AKT1/AKT2 double knock-out (DKO) MEF (mouse embryo fibroblast) cell was kindly provided by Dr. Navdeep S. Chandel (Division of Pulmonary and Critical Care Medicine, Feinberg School of Medicine, Northwestern University). JNK1$^{-/-}$ and JNK2$^{-/-}$ MEF cells were kindly provided by Dr. Jing Liu (Division of Pulmonary and Critical Care Medicine, Feinberg School of Medicine, Northwestern University). A549 cells were cultured in DMEM supplemented with 10% heat-inactivated fetal bovine serum, penicillin (50 units/ml), and streptomycin (50 units/ml). The cells were incubated at 37°C with humidified 5% CO^2, and seeded at a concentration of 1.5×10^5 in 6-well plate. For chrysotile asbestos experiments, cells were treated with chrysotile asbestos at the concentration of 100 μg/cm^2 for different time periods as indicated as follows in 5% FBS supplemented medium. For the studies testing the effects of inhibitors, A549 cells were pretreated for 1h with inhibitors such as 3-MA(Sigma, 10 mM), E64d(Merk, 10 μg/ml), pepstatin A1(Merk, 10 μg/ml), SB203580 (Merk, 10 μM), N-acetyl cysteine (NAC) (Sigma-Aldrich, 5 mM), pifithrin-α (PFT-α) (Merk, 30 μM) and then treated with chrysotile asbestos in the presence of the inhibitors. Inhibitors were dissolved in dimethyl sulfoxide (DMSO) and the final concentrations of DMSO in the culture medium did not exceed 0.2%.

Cell death assay

For cell death evaluation, the treated cells were stained with 0.25% trypan blue solution and then counted using a hemacytometer (Neubauer Improved, Marienfeld, Germany) under a light microscope.

Acridine orange staining and MDC incorporation assay

A549 cells were treated with chrysotile asbestos (50, 100, 150, 200, 300 μg/cm^2) for 5h or with chrysotile asbestos at 100 μg/cm^2 for different time durations (1 h, 3 h, 5 h). After rinsing with fresh medium, the cells were stained with 1 μg/mL of acridine orange solution at 37°C for 15 minutes, and the fluorescence signal was examined using a confocal microscope (Leica TCS SP5 II, Germany) with a peak excitation wavelength of 490nm. MDC staining of autophagic vacuoles (AVOs) was also performed for autophagy analysis. Cells were treated with chrysotile asbestos (50, 100, 150, 200, 300 μg/cm^2) for 5 h or with chrysotile asbestos at 100 μg/cm^2 for 1 h, 3 h, 5 h. Then autophagic vacuoles were labeled with 0.05 mM MDC in PBS at 37°C for 10 min. After incubation, the cells were washed three times with PBS and immediately analyzed under a confocal laser scanning microscope (Leica TCS SP5 II, Germany). Fluorescence of MDC was measured at the excitation wavelength 380 nm with an emission filter at 530 nm.

Transmission electron microscopy

A549 cells were treated with 100 μg/cm^2 chrysotile asbestos for 24 h. For the sample preparation, cells were fixed in 2.5% glutaraldehyde in PBS (pH 7.4). Samples were further fixed with 1% osmium tetroxide for 1hr, serially dehydrated with ethanol, and embedded in epoxy resin. For transmission electron microscopy (TEM), sections (70 nm) were cut on a

Leica Ultra-CUT (Ultra-Microtome, Leica Microsystems GmbH, Wetzlar, Germany) and contrasted with 0.1% lead citrate and 8% uranyl acetate in 50% EtOH. Ultrathin sections were examined with a transmission electron microscope (JEM-1400 Transmission Electron Microscope, Japan) operated at 120 kV, and the images were captured with a Megaview III CCD camera (Soft Imaging System, Lakewood, CO). A cell showing two or more autophagosomes was defined to be an autophagy-positive cell. To examine the distribution of LC3 in A549 cells, images were taken and processed with confocal microscope (Leica TCS SP5 II, Germany).

Transient transfection and small interfering RNA (SiRNA)

The EGFP-mCherry-LC3 fusion plasmid was purchased from Biovector Science Lab, Inc. A549 cells were plated at a density of 2×10^5 on a confocal dish and cultured up to 60% confluence. Transfection was carried out with Lipofectamine 2000 as manufacturer's recommendation and 2 μg/ml plasmid DNA in each dish was used. When cells reached 90% confluence in DMEM containing 10% FBS medium, chrysotile asbestos was added into culture medium for 24 h. For siRNA, ATG5 siRNA was transfected according to manufacturer's protocol.

Immunofluorescence staining and Fluorescence Microscopy

For treatment, cells were enzymatically removed from the flasks and plated in 35 mm diameter confocal dish (Coverglass-Bottom Dish). After 24 h in culture, the medium was changed to 2 ml of fresh medium with chrysotile asbestos fibers at an approximate final concentration of 100 $\mu g/cm^2$. The fibers remained in contact with the cells for a period of 24 h, after which the medium was changed. After additional periods of 24 h, cells were washed with PBS three times and fixed with 3.7% formaldehyde for 30 min. In all the treatment conditions, the medium culture used was supplemented with 10% fetal bovine serum. Nonspecific binding was blocked by incubating the coverslip with 5% normal donkey serum in 1% BSA in PBS for 15 min at room temperature followed by incubation for 90 min with 1% BSA in PBS containing primary antibodies: rabbit anti-LC3 (1:200 dilutions). Dishes were washed with PBS for three times at 5 min each wash, and then labeled with a 1:500 dilution of donkey anti-rabbit Alexa-Fluor 488 for 30 min at room temperature in dark. For visualization of nuclei, coverslips were stained with DAPI at 1:5,000 dilutions in PBS for 2 min. Subsequently, dishes were mounted with Prolong Gold Antifade Reagent, and fluorescent images were captured using laser confocal microscope (Leica TCS SP5 II, Germany). The images were prepared and labeled using Adobe Photoshop 7.0 software. To analyze autophagic flux, A549 cells were transfected with mCherry-EGFP-LC3 expressing plasmid. Cells were pooled, seeded in chamber slides and left untreated (to avoid transfection-induced autophagy). Autophagic flux was determined by evaluating the punctate pattern of EGFP and mCherry (puncta/cell were counted). Fluorescence images were obtained on laser confocal microscope (Leica TCS SP5 II, Germany) and analyzed using the Cell M software.

Cell lysis, SDS-PAGE and Western Blot analysis

Cells were lysed on ice for 15 min in 1xRIPA lysis buffer. Protein concentration was measured using a BCA kit (Beyotime, China). Equal amounts of cell extracts were boiled

for 5 min in the presence of 1% 2-mercaptoethanol and 2% sodium dodecyl sulfate (SDS). Soluble proteins were isolated from the untreated or treated A549 cells for Western blotting. Equal amounts of protein (20 μg) from each sample were separated by electrophoresis through a 8%–12% SDS-polyacrylamide gel, transferred to polyvinylidene difluoride membranes, and blocked with 5% nonfat dry milk in 1×TBS plus 0.1% Tween 20 at room temperature for 1 h. The membranes were incubated overnight at 4°C with a primary antibody diluted in 5% nonfat dry milk in 1×TBS plus 0.1% Tween-20. The primary antibody against actin (diluted 1:5000) was purchased from Cell Signaling Technology (Beverly, MA). The membranes were washed and incubated again for 1h at room temperature with a horseradish peroxidase conjugated anti-mouse or anti-rabbit secondary antibody. The bound antibody was detected using an enhanced chemiluminescence reagent (Enhanced Chemiluminescence Western blotting system, Amersham Biosciences Corp., Piscataway, NJ).

Real-time-PCR for mRNA quantification

Total RNA was extracted using the TRIzol reagent (Invitrogen, USA), and cDNA was prepared using 0.5 μg of oligo-d (T) primers and the PrimeScript RT reagent (Takara Bio, Japan) according to the manufacturer's protocol. Real time quantitative PCR (QRT-PCR) analysis was performed using SYBR Green assays (Takara Bio, Japan) on the following genes: LC3 using the following primers: LC3, sense 5′-AAACGCATTTGCCATCACAGT-3′ and antisense 5′-GTGAGGACTTTGGGTGTGGTTC-3′; GAPDH, sense 5′-AGAAGGCTGGGGCTCATTTG-3′ and antisense 5′-AGGGGCCATCCACAGTCTTC-3′. Each test was carried out in triplicate according to standard protocol. Data were calculated using the 2Δ ΔCt method comparing ΔCt of treated A549 cells to ΔCt control untreated samples. Reactions were incubated in the LightCycler® 480 Real-Time PCR System. Ct values were calculated using the SDS software version 2.3 applying automatic baseline and threshold settings.

Analysis of intracellular ROS levels

ROS production in A549 cells was separately measured by flow cytometry with the fluorescent dye dihydroethidium (DHE) and Amplex Red that have been used to quantify the intracellular oxidant production [23,24]. A549 cells were grown on 12-well plates. Intracellular O_2^- generation was monitored by measuring the change of fluorescence caused by oxidation of intracellular DHE. DHE enters the cells and is oxidized by O_2^- or ·OH to yield the red fluorescent ethidium, which then binds to DNA, causing amplification of the red fluorescence signal. DHE (50 μM) was added to the cell suspension in PBS for 30 min after each experiment, and the fluorescence was determined with a FACScan (BD FACS Canto II, CA, USA) flow cytometry equipped with a 488-nm argon ion laser and supplied with Cell Quest software. DHE fluorescence was measured using 488-nm excitation, and emission was measured using a 585 ± 42 nm band-pass filter. For Amplex Red assay, A549 cells were grown on 12-well plates, 24 h later, cells were washed once with phosphate-buffered saline (PBS) and subsequently incubated in PBS containing 50 μM Amplex Red and 0.25 units/ml HRP. After 30 min, the supernatant was transferred to a 96-well plate, and

H_2O_2-dependent oxidation of Amplex Red was measured with a FACScan (BD FACS Canto II, CA, USA) flow cytometer (excitation 540 nm, emission 580 nm).

Statistical analysis

The data including Fig. 2 – Fig. 6 and Fig S1–Fig S5 were expressed as the mean ± SEM of at least three independent experiments, statistical analysis was performed using one-way analysis of variance (ANOVA) followed by Bonferroni's multiple comparison test. Statistical calculations were performed using GraphPad Prism (GraphPad, San Diego, CA, USA). **P*-value <0.05, ***P*-value <0.01, ****P*-value <0.001 were considered statistically significant.

Results

Chrysotile Asbestos Induces the Formation of Autolysosomes and the Accumulation of Acidic Vesicles in A549 Cells

The formation of autolysosomes and accumulation of acidic vesicles, which are revealed by lysosomotropic agent acridine orange (AO) and monodansylcadaverine (MDC), respectively, are two markers of autophagy. Red AVOs were formed in the presence of chrysotile asbestos in a dose- and time-dependent manner, as shown in Fig. 1A–B. A moderate concentration (100 μg/cm^2) of chrysotile asbestos was selected according to the results of Trypan blue dye exclusion assay (data not shown). Cells treated with chrysotile asbestos for 1–5 h resulted in the formation of red AVOs, which were rare in PBS-treated control cells (Fig. 1B, Left panel) but comparable rapamycin-treated cells (Fig. 1B, Middle panel), our positive control. Monodansylcadaverine (MDC) staining was also used to detect autophagic vacuoles because of accumulation of monodansylcadaverine in mature autophagic vacuoles, such as autophagolysosomes. As shown in Fig. 1A and C, in agreement with the results of AO staining, the accumulation of monodansylcadaverine in the A549 cells treated with chrysotile asbestos from one to five hour was apparent, and compared with the control, the blue color in treated cells was brighter, whereas the control A549 cells did not exhibit noticeable accumulation of monodansylcadaverine.

To determine whether chrysotile asbestos induces autophagy in lung cancer cells, we examined the intracellular distribution of microtubule-associated protein1 light chain 3 (LC3), an autophagy marker [25], by immunofluorescence upon chrysotile asbestos treatment of A549 cells. As shown in Fig. 1D, a change in the distribution of LC3 fluorescence from a diffuse cytosolic pattern in PBS-treated cells to a punctate pattern upon chrysotile asbestos treatment was observed. When these chrysotile asbestos-treated cells were examined under a transmission electron microscope, double-membrane structures containing high-electron-density substances characteristic of autophagosomes and autolysosomes were detected (Fig. 1E).

Chrysotile Asbestos Induces Autophagy in A549 Cells

Furthermore, we analyzed the expression of microtubule-associated protein 1 light chain 3 (LC3) at the protein level using Western blot analysis and at the mRNA level using QRT-PCR. LC3-II is an important protein marker for autophagic activity [26]. We detected a 1.5-

to 2.2-fold increase in LC3-II in chrysotile asbestos-treated cell lysates as early 30 min and this level of expression persisted for over 24 h, as shown in Fig. 2A. Chrysotile asbestos incubation induced a time-dependent protein accumulation of LC3-II in A549 cells which appeared at 0.5–24 h and an increase in the mRNA level of LC3 in A549 cells as early as 1 h (Fig. 2B). Collectively, these results provide evidence that chrysotile asbestos induces autophagy in A549 cells.

Autophagy is a dynamic process that includes autophagosome formation and degradation defined as autophagic flux [27]. We then examined whether there was sufficient autophagic flux upon exposure to chrysotile asbestos. Autophagic flux is crucial in determining whether the autophagic cargo and assembly reach the lysosomes and for degradation [28]. Therefore, we investigated the effect of co-administration lysosomal inhibition (E64d+pepstain A) and chrysotile asbestos on LC3-II formation (Fig. 2C). Our results showed that the inhibitors increased LC3-II turnover in the cells at early time points (4 h).

Tandem fluorescent-tagged LC3 reporters (mCherry-EGFP-LC3) have been widely used for monitoring autophagic flux in live cells [29]. In order to monitor the process of autophagosome maturation, we generated A549 cells transfected with the tandem tagged, fluorescent reporter mCherry-EGFP-LC3-II. This reporter consists of a fusion protein of the fluorescent proteins mCherry, enhanced green fluorescent protein (EGFP) and microtubule-associated 1 light chain 3 isoform b (LC3-II), a membrane associated marker of autophagic vesicles. At neutral pH, both mCherry and EGFP emit fluorescence and LC3-positive vesicles appear yellow in merged images. In green/red merged images, yellow puncta (i.e., RFP^+GFP^+) indicate autophagosomes, while red puncta (i.e., RFP^+GFP^-) indicate autolysomes. Autophagic flux is increased when both yellow and red puncta are increased in asbestos treated-cells (Fig. 2D). These findings indicate that chrysotile asbestos enhanced the autophagic flux.

Chrysotile Asbestos Augments Autophagy through the AKT-mediated Inhibition of mTORC1 and p70S6K in A549 Cells

It has been reported that PI3K/AKT/mTOR signaling plays an important role in cell proliferation and autophagy. The impact of chrysotile asbestos on PI3K/AKT/mTOR activity was investigated next. As shown in Fig. 3, chrysotile asbestos significantly down-regulated the level of phospho-AKT (ser473) (Fig. 3A). To examine the role of mTOR in chrysotile asbestos-reduced autophagy, we examined the phosphorylation levels of mTOR and p70S6K, one of the two best characterized targets of mTOR. Our results showed that chrysotile asbestos had no effect on the total protein level of mTOR and p70S6K, but inhibited the phosphorylation level of mTOR and p70S6K (Fig. 3B–C). However, when AKT (DKO) MEF cells were treated with chrysotile asbestos, autophagy induced by chrysotile asbestos was abolished compared with the WT MEF cells treated with chrysotile asbestos alone (Fig. 3D).

JNK but Not p38 MAPK Signaling Mediates Chrysotile Asbestos-Induced Autophagy

To investigate the role of the MAPK pathway in chrysotile asbestos-induced autophagy, the activation of JNK, ERK and p38 MAPK were examined by Western blot using

phosphorylated antibodies specific for the active form of these enzymes. p38 MAPK and JNK were activated in a time-dependent manner (Fig. 4A, D). However, ERK was not activated (Fig. 4C). To further investigate the role of p38 MAPK and JNK in chrysotile asbestos-induced autophagy, SP600125, an inhibitor of JNK, was used and observed to block chrysotile asbestos-induced LC3-II protein accumulation (Fig. 4E). SB203580, an inhibitor of p38 MAPK, did not block autophagy induced by chrysotile asbestos (Fig. 4B). When JNK1$^{-/-}$ and JNK2$^{-/-}$ MEF cells were treated with chrysotile asbestos, LC3-II was abolished in JNK2$^{-/-}$ MEF cells, but not in JNK1$^{-/-}$ MEF cells. These results demonstrated that JNK2 signaling pathway is required in chrysotile asbestos-induced autophagy.

ROS and p53 Are Involved in Chrysotile Asbestos-Induced Autophagy

Having established the ability of chrysotile asbestos to induce autophagy in A549 cells, we set out to investigate the molecular mechanism underlying this biological event, since ROS generation is prominently implicated in mediating toxicity by chrysotile asbestos [30–32]. We assessed chrysotile asbestos-induced ROS production in A549 cells by using flow cytometry with DHE and Amplex Red to evaluate the production of superoxide anions and the release of hydrogen peroxide. We find that chrysotile asbestos caused a dose- and time-dependent increase in ROS production (Fig. S3 A–B and Fig S4 A–B). We sought to determine the role of ROS-mediated signaling in chrysotile asbestos-induced autophagy in A549 cells. As shown in Fig. S3C and S4C, NAC (5 mM) attenuated chrysotile asbestos-induced ROS production as compared with chrysotile asbestos alone. To determine whether chrysotile asbestos-induced ROS mediate the dephosphorylation of p-AKT, we examined p-AKT level utilizing western blot in non-treated cells and in cells pre-incubated for 1 h with or without NAC (5 mM) followed by treatment by 100 μg/cm^2 chrysotile asbestos for 24 h. Fig. S5 show that the dephosphorylation of p-AKT by chrysotile asbestos was partly reversed by NAC. On the other hand, ROS also are regulators of mitogen-activated protein kinase (MAPK), a family of serine/threonine kinases which mediates intracellular signal transduction in response to different physiological stimuli and stress conditions, to verify whether chrysotile asbestos-induced ROS activates p-JNK, we tested p-JNK level using western blot in non-treated cells and in cells pre-incubated for 1 h in the presence or absence of NAC, followed by exposure to 100 μg/cm^2 chrysotile asbestos for 24 h. Fig. 5A shows that the activation of JNK by chrysotile asbestos was significantly diminished by NAC. The data strongly suggests that intracellular chrysotile asbestos-induced autophagy was dependent on ROS in this model, and that in part, ROS is upstream of JNK signaling pathway.

Since p53 can regulate autophagy and apoptosis, we next suppressed p53 activity in A549 cells using the chemical inhibitor of p53, cyclic pifithrin-α, and measured the impact of this on autophagy induced by chrysotile asbestos in A549 cells. As shown in Fig. 5B, LC3-II formation was reduced in the presence of p53 inhibitor. These data showed that chrysotile asbestos-induced autophagy is p53-dependent in A549 cells.

Chrysotile Asbestos-Induced Autophagy Is Apoptosis-Independent in A549 Cells

To test whether autophagy is an integral part of chrysotile asbestos-induced cell death, we measured cell survival in the presence of 3-MA or knockdown of ATG5 (autophagy-related

gene 5). First, as shown in Fig. 6, active caspase-9 was detected by immunofluorescence staining after chrysotile asbestos treatment of A549 cells supporting the activation of mitochondria-regulated apoptosis similar to what we have reported following exposure to amosite asbestos[2, 4, 19, 20]. The effects of 3-MA on cell survival are shown in Fig. 6A–C. Compared to controls, 3-MA alone modestly augmented cell death but not apoptosis; further 3-MA did not significantly affect apoptosis or cell death following exposure to chrysotile asbestos for 24 h. A549 cells transfected with shRNA for ATG5 in the presence or absence of chrysotile asbestos, reduced the level of LC3-II expression by 41% and 66%, respectively (Fig. 6D). In addition, the proportion of cell death following chrysotile exposure was similar between the control cells and the ATG5 knockdown cells as assessed by trypan blue dye exclusion (Fig. 6E). Taken together, these results indicate that autophagy induction by chrysotile asbestos does not protect cells from death, and that chrysotile asbestos-induced autophagy is apoptosis-independent in A549 cells.

Discussion

Asbestos-induced pulmonary toxicity is mediated in part by lung epithelial cell injury by mechanisms that are not fully understood [2, 4, 5, 19]. Accumulating evidence implicates autophagy-dependent mechanisms in the pathogenesis of several pulmonary diseases but whether autophagy is important following asbestos exposure is unknown [9, 14]. The major findings of this study are that chrysotile asbestos induces autophagy in human A549 lung epithelial cells as well as MEF as assessed using a variety of biochemical and histologic criteria. Further, we show that asbestos-induced autophagy is mediated in part by inhibition of AKT/mTOR signaling and activation of the JNK2 and p53. Overall, these results suggest several novel signaling pathways that may be relevant in the pathophysiology of asbestos-related pulmonary diseases.

An important finding of this study is that chrysotile asbestos causes autophagy in both human A549 cells as well as in MEF. We document asbestos-induced autophagy by several techniques including (1) the formation of AVOs and autophagosomes as assessed by immunofluorescence and electron microscopy (Fig. 1) and (2) increased LC3-II mRNA and protein expression (Fig. 2). Immunoflourescence studies demonstrated that the levels of asbestos-induced autophagy were similar to that caused by rapamycin, a well known activator of autophagy that occurs by inhibiting mTOR (Fig. 1). Our findings with asbestos are in accord with others showing that various toxins cause autophagy in A549 cells, an alveolar type 2-like epithelial lung cancer cell line with wild-type p53 function [4, 33–36]. Although we focused on human A549 cells in this study, we previously reported that amosite asbestos-induced mitochondrial dysfunction, DNA damage, p53 activation and mitochondria-regulated apoptosis are all comparable in A549 and primary isolated rat alveolar type 2 cells [37, 38]. Additional studies examining the role of asbestos-induced autophagy in primary isolated lung epithelial cells as well as the relevance of these findings using *in vivo* rodent models will be of interest in future studies.

Previous studies have established that reduced signaling via the AKT/mTOR patways are involved in activating autophagy [8, 9, 39]. Several lines of evidence presented in this study support the role of the AKT/mTOR pathway in mediating chrysotile asbestos-treated

autophagy. First, as shown in Fig. 1, our findings with asbestos parallel that of rapamycin, the mTOR inhibitor and 'classical' autophagy suppressor [40]. Second, we observed that asbestos augmented A549 cell LC3-II mRNA and protein expression in conjunction with dephosphorylation of phospho-AKT, phospho-mTOR, and phospho-P70s6k (Fig. 3). Reduced phosphorylation of AKT and mTOR was observed after chrysotile-treatment as early as 0.5 h and persisted for 5 h. Finally, AKT1/AKT2 double knockout (AKT DKO) murine embryonic fibroblasts (MEFs) had negligible asbestos-induced LC3-II expression supporting a crucial role for AKT signaling. Furthermore, in AKT1/AKT2 double knock-out (DKO) MEF cells, the expression of LC3-II was blocked entirely, indicating that AKT mediates chrysotile asbestos-induced autophagy in our model. Collectively, these results suggest that the effect of chrysotile asbestos on autophagy is mediated at least in part via inhibition of AKT/mTOR signaling pathways.

In mammalian cells, ROS are important regulators of autophagy under various conditions [41, 17]. Studies in yeast indicate that mitochondrial oxidative stress plays a crucial role in the induction of autophagy [42]. Oxidative stress from H_2O_2 and hydroxyl radicals (•OH) are prominently implicated in the pathobiology underlying the *in vivo* and *in vitro* toxic effects of inhaled asbestos [18, 43, 45]. Although ROS can induce autophagy through several distinct mechanisms, it is unclear whether asbestos-induced free radical production mediates autophagy in lung epithelial cells [16]. ROS can directly induce dephosphorylation of mTOR and p70 ribosomal protein S6 kinase in a Bcl-2/E1B 19 kDa interacting protein 3 (BNIP3)-dependent manner in C6 glioma cells [46]. Using flow cytometry with the fluorescent dye DHE and Amplex Red to quantify intracellular oxidant production induced by chrysotile asbestos in A549 cells, we observed a dose- and time-depenednt mechanism (Fig. S3 A, B and Fig. S4 A, B). In our study, we found that NAC attenuated chrysotile asbestos-induced dephosphorylation of AKT in A549 cells (Fig. S5) and blocked phospho-JNK activation (Fig. 5A). Our findings are in accord with others showing that NAC markedly inhibits autophagy and Akt-mTOR signaling in some cancer cells [17, 47]. Collectively, our data show that chrysotile asbestos-induced autophagy in A549 cells is mediated in part through a ROS-dependent mechanism. However, the detailed molecular mechanisms involved await further studies.

Asbestos can alter signaling pathways involving epithelial cell plasticity including the class III PI3K and MAPK family members such as ERK, p38, and JNK [48]. Although unclear with asbestos fibers, ROS-dependent JNK activation occurs following exposure to various stimuli that subsequently regulate fundamental cellular pathways such as autophagy and apoptosis [49]. ROS that are produced endogenously by deranged metabolism of cancer cells, or exogenously by ROS-generating drugs, can promote autophagy in part via signaling pathways involving JNK, ERK, p38, and p53 [20, 49, 50]. Several groups have reported that ROS-dependent ERK and/or JNK signaling pathways activate autophagy in part by inducing Beclin 1 expression that promotes the conversion of LC3-I to LC3-II [14, 51–53]. Herein, we report that chrysotile asbestos reduces phospho-ERK and activates phosph-p38 and phospho-JNK signaling pathways in A549 cells (Fig. 4). An innovative finding from this study is that using pharmacologic as well as genetic approaches we show that JNK2 signaling is important for mediating asbestos-induced autophagy (Fig. 4). We demonstrated

that the JNK inhibitor SP600125 significantly abolished chrysotile asbestos-induced autophagy (Fig. 4E). Notably, chrysotile asbestos-induced autophagy as assessed by LC3-II expression was abolished in JNK2$^{-/-}$ MEF cells but not in JNK1$^{-/-}$ MEF cells (Fig. 4F). MAPK pathway also transduce signals in other cascades, creating a crosstalk and a wide intracellular network, to explore the AKT and MAPK cascade communicate with each other in response to chrysotile asbestos, we investigated the effect on the absence of Akt in response to chrysotile asbestos on both JNK and P38 (Fig. S1), the results is that both JNK and P38 is not significantly changed, although some reports showed AKT is able to phosphorylate and inhibit the activity of ASK1 and MLK3 that belong to the MAPKKK upstream activation of JNK [57]; Reversely, we also experimentally assessed the response of AKT in inhibition of both JNK and p38, we found the inhibition of JNK but not p38, leads chrysotile asbestos-induced AKT dephosphorylation, the fact that inhibited JNK exhibit phosphorylation of P-AKT suggests that many other targeted protein mediated the signaling remain to be identified, the complexity of P38 and JNK signaling in A549 cells may be inferred involving in intriguing network [55, 56]. Collectively, these results indicate a key role for JNK2 signaling in mediating chrysotile asbestos-induced autophagy and AKT/mTOR and MAPKs signaling pathway are in complex crosstalk network, more work is needed to do in this signaling network [55], and that ROS are crucial in asbestos-induced phosphorylation of JNK.

Depending on the cell type as well as the strength and duration of the stress stimuli, autophagy can either promote or inhibit cancer cell death [8, 9, 57]. The molecular mechanisms of this double role of autophagy are not clear. We observed that pifithrin-alpha, an inhibitor or p53-dependent transcription that we previously showed completely abolishes asbestos-induced mitochondrial dysfunction and intrinsic A549 cell apoptosis [58], completely prevented chrysotile-induced autophagy (Fig. 5B). Our findings with asbestos are in accord with studies showing that p53 mediates LC3 expression during prolonged starvation [50]. Further, p53 plays a critical role in autophagy and metabolism via effects on mitochondrial respiration [59]. Interestingly, we noted that blocking autophagy with either pharmacological inhibitors (3-MA) or siRNA targeting a key autophagy factor, ATG5, did not affect chrysotile asbestos-induced apoptotic cell death (Fig. 6). Taken together, our findings indicate that apoptosis of A549 cells exposed to chrysotile asbestos is autophagy-independent. This suggests that autophagy is playing an adaptive role in our model. The data in Fig 6 also support an adaptive response for autophagy rather than a prosurvival response in our model. Further, the role of autophagy in regulating cancer cell survival and apoptosis is complex. Future studies will be necessary to characterize the various specific autophagic signaling pathways activated by asbestos (e.g. macroautophagy, microautophagy, and/or chaperone-mediated autophagy) in both primary isolated lung epithelial cells as well as in specific malignant cell types. We acknowledge that chrysotile asbestos-induced autophagy in A549 cells *in vitro* is not reflective of conditions *in vivo* particularly in the context of human disease, but we reason that asbestos-induced autophagy may be an early adaptive response following lung fiber exposure. Autophagy may either promote adaptive cellular responses or cell death (apoptosis) depending on many factors. Additional studies will be of considerable interest further characterizing the molecular mechanisms driving asbestos-

induced autophagy and apoptosis in the context of health and disease (pulmonary fibrosis and malignant transformation).

In summary, we show that chrysotile asbestos stimulates autophagy in human lung epithelial cells (A549) as well as MEF as assessed using ultrastructural and biochemical features characteristic of autophagy. This study also demonstrates that chrysotile-induced autophagy is associated with altered signaling via the AKT/mTOR and JNK2 pathways but independent of apoptosis. On the other hand, there are an effect of interaction between AKT/mTOR and JNK signaling pathway in presence of chrysotile asbestos. Moreover, chrysotile asbestos-induced autophagy is mediated in part by ROS- and p53-dependent mechanisms. However, the detailed molecular mechanisms involved as well as the in vivo significance await further study. Our study provides a mechanistic basis for possible future clinical applications targeting these signaling pathways in the management of asbestos-induced lung disease as well as other degenerative (e.g. COPD and IPF) and malignant diseases for which novel treatments are needed.

Supplementary Material

Refer to Web version on PubMed Central for supplementary material.

Acknowledgments

This work was supported by the Natural Science Foundation of China project 81172615, STIF201109, VA Merit (DK) and RO1ES020357 (DK). The funders had no role in study design, data collection and analysis, decision to publish, or preparation of the manuscript. We thank Hai-Li Huang, Yan-li Cai for technical assistance.

References

1. Mossman BT, Kamp D, Weitzman SA. Mechanisms of carcinogenesis and clinical features of asbestos-associated cancers. Cancer Invest. 1996; 14:464–478.
2. Kamp DW. Asbestos-induced lung diseases: an update. Translational Research. 2009; 153:143–152. [PubMed: 19304273]
3. Cugell DW, Kamp DW. Asbestos and the PleuraA Review. CHEST Journal. 2004; 125(3):1103–1117.
4. Liu G, Kamp DW. Molecular Basis of Asbestos-Induced Lung Disease. Annual Review of Pathology: Mechanisms of Disease. 2013; 8:161–187.
5. Mossman BT, Churg A. Mechanisms in the pathogenesis of asbestosis and silicosis. American journal of respiratory and critical care medicine. 1998; 157:1666–1680. [PubMed: 9603153]
6. Zanella CL, Posada J, Tritton R, Mossman BT. Asbestos causes stimulation of the extracellular signal-regulated kinase 1 mitogen-activated protein kinase cascade after phosphorylation of the epidermal growth factor receptor. Cancer research. 1996; 56(23):5334–5338. [PubMed: 8968079]
7. Baldys A, Pande P, Mosleh T, Park S-H, Aust AE. Apoptosis induced by crocidolite asbestos in human lung epithelial cells involves inactivation of AKT and MAPK pathways. Apoptosis. 2007; 12:433–447. [PubMed: 17191120]
8. Rubinsztein DC, Codogno P, Levine B. Autophagy modulation as a potential therapeutic target for diverse diseases. Nature Reviews Drug Discovery. 2012; 11(9):709–730.
9. Margaritopoulos GA, Tsitoura E, Tzanakis N, Spandidos DA, Siafakas NM, Sourvinos G, Antoniou KM. Self-Eating: Friend or Foe? The Emerging Role of Autophagy in Idiopathic Pulmonary Fibrosis. BioMed research international. 2013:2013.
10. Virgin HW, Levine B. Autophagy genes in immunity. Nature immunology. 2009; 10:461–470. [PubMed: 19381141]

11. Nakahira K, Haspel JA, Rathinam VA, Lee S-J, Dolinay T, Lam HC, Englert JA, Rabinovitch M, Cernadas M, Kim HP. Autophagy proteins regulate innate immune responses by inhibiting the release of mitochondrial DNA mediated by the NALP3 inflammasome. Nature immunology. 2010; 12:222–230. [PubMed: 21151103]
12. Shi C-S, Shenderov K, Huang N-N, Kabat J, Abu-Asab M, Fitzgerald KA, Sher A, Kehrl JH. Activation of autophagy by inflammatory signals limits IL-1[beta] production by targeting ubiquitinated inflammasomes for destruction. Nat Immunol. 2012; 13:255–263. [PubMed: 22286270]
13. Levine B. Cell biology: autophagy and cancer. Nature. 2007; 446:745–747. [PubMed: 17429391]
14. Choi AJ, Ryter SW. Autophagy in inflammatory diseases. International journal of cell biology. 2011:2011.
15. Yousefi S, Perozzo R, Schmid I, Ziemiecki A, Schaffner T, Scapozza L, Brunner T, Simon HU. Calpain-mediated cleavage of Atg5 switches autophagy to apoptosis. Nature cell biology. 2006; 8:1124–1132.
16. Azad MB, Chen Y, Gibson SB. Regulation of autophagy by reactive oxygen species (ROS): implications for cancer progression and treatment. Antioxidants & redox signaling. 2009; 11(4): 777–790. [PubMed: 18828708]
17. Li Z, Yang Y, Ming M, Liu B. Mitochondrial ROS generation for regulation of autophagic pathways in cancer. Biochemical and biophysical research communications. 2011; 414(1):5–8. [PubMed: 21951851]
18. Mossman BT, Marsh JP. Evidence supporting a role for active oxygen species in asbestos-induced toxicity and lung disease. Environmental health perspectives. 1989; 81:91. [PubMed: 2667992]
19. Kamp DW, Weitzman SA. The molecular basis of asbestos induced lung injury. Thorax. 1999; 54:638–652. [PubMed: 10377212]
20. Liu G, Beri R, Mueller A, Kamp DW. Molecular mechanisms of asbestos-induced lung epithelial cell apoptosis. Chemico-biological interactions. 2010; 188:309–318. [PubMed: 20380827]
21. Timbrell V, Gibson J, Webster I. UICC standard reference samples of asbestos. International Journal of Cancer. 2006; 3:406–408.
22. Hei TK, Piao CQ, He ZY, Vannais D, Waldren CA. Chrysotile fiber is a strong mutagen in mammalian cells. Cancer research. 1992; 52(22):6305–6309. [PubMed: 1330290]
23. González-Perilli L, Álvarez MN, Prolo C, Radi R, Rubbo H, Trostchansky A. Nitroarachidonic acid prevents NADPH oxidase assembly and superoxide radical production in activated macrophages. Free Radical Biology and Medicine. 2013; 58:126–133. [PubMed: 23318789]
24. Haugen TS, Skjonsberg OH, Kahler H, Lyberg T. Production of oxidants in alveolar macrophages and blood leukocytes. European Respiratory Journal. 1999; 14(5):1100–1105. [PubMed: 10596697]
25. Kabeya Y, Mizushima N, Ueno T, Yamamoto A, Kirisako T, Noda T, Kominami E, Ohsumi Y, Yoshimori T. LC3, a mammalian homologue of yeast Apg8p, is localized in autophagosome membranes after processing. EMBO J. 2000; 19:5720–5728. [PubMed: 11060023]
26. Kothakota S, Azuma T, Reinhard C, Klippel A, Tang J, Chu K, McGarry TJ, Kirschner MW, Koths K, Kwiatkowski DJ. Caspase-3-generated fragment of gelsolin: effector of morphological change in apoptosis. Science. 1997; 278:294–298. [PubMed: 9323209]
27. Kimura S, Fujita N, Noda T, Yoshimori T. Monitoring autophagy in mammalian cultured cells through the dynamics of LC3. Methods in enzymology. 2009; 452:1–12. [PubMed: 19200872]
28. Iwai-Kanai E, Yuan H, Huang C, Sayen MR, Perry-Garza CN, Kim L, Gottlieb RA. A method to measure cardiac autophagic flux in vivo. Autophagy. 2008; 4(3):322–329. [PubMed: 18216495]
29. Tresse E, Salomons FA, Vesa J, Bott LC, Kimonis V, Yao TP, Dantuma NP, Taylor JP. VCP/p97 is essential for maturation of ubiquitin-containing autophagosomes and this function is impaired by mutations that cause IBMPFD. Autophagy. 2010; 6:217–227. [PubMed: 20104022]
30. Elstner EF, Schutz W, Vogl G. Enhancement of enzyme-catalyzed production of reactive oxygen species by suspensions of “crocidolite” asbestos fibres. Free Radical Research. 1986; 1(6):355–359.

31. Mossman BT, Marsh JP, Shatos MA, Doherty J, Gilbert R, Hill S. Implication of active oxygen species as second messengers of asbestos toxicity. Drug and chemical toxicology. 1987; 10(1–2): 157–180. [PubMed: 2824166]
32. Kamp DW, Graceffa P, Pryor WA, et al. The role of free radicals in asbestos-induced diseases. Free Radical Biology and Medicine. 1992; 12(4):293–315. [PubMed: 1577332]
33. Chen MC, Chen CH, Liu YN, Wang HP, Pan SL, Teng CM. TW01001, a novel piperazinedione compound, induces mitotic arrest and autophagy in non-small cell lung cancer A549 cells. Cancer letters. 2013; 336(2):370–378. [PubMed: 23567646]
34. Pan X, Zhang X, Sun H, Zhang J, Yan M, Zhang H. Autophagy Inhibition Promotes 5-Fluorouraci-Induced Apoptosis by Stimulating ROS Formation in Human Non-Small Cell Lung Cancer A549 Cells. PloS one. 2013; 8(2):e56679. [PubMed: 23441212]
35. Wang W, Fan H, Zhou Y, Duan P, Zhao G, Wu G. Knockdown of autophagy-related gene BECLIN1 promotes cell growth and inhibits apoptosis in the A549 human lung cancer cell line. Molecular medicine reports. 2013; 7:1501–1505. [PubMed: 23525201]
36. Deng X, Zhang F, Rui W, Long F, Wang L, Feng Z. PM2.5-induced Oxidative Stress Triggers Autophagy in Human Lung Epithelial A549 Cells. Toxicology in Vitro. 2013; 27(6):1762–1770. [PubMed: 23685237]
37. Kamp DW, Israbian VA, Preusen SE, Zhang CX, Weitzman SA. Asbestos causes DNA strand breaks in cultured pulmonary epithelial cells: role of iron-catalyzed free radicals. American Journal of Physiology-Lung Cellular and Molecular Physiology. 1995; 268:471–480.
38. Panduri V, Weitzman SA, Chandel N, Kamp DW. The mitochondria-regulated death pathway mediates asbestos-induced alveolar epithelial cell apoptosis. American journal of respiratory cell and molecular biology. 2003; 28(2):241–248. [PubMed: 12540492]
39. Aoki H, Takada Y, Kondo S, Sawaya R, Aggarwal BB, Kondo Y. Evidence that curcumin suppresses the growth of malignant gliomas in vitro and in vivo through induction of autophagy: role of AKT and extracellular signal-regulated kinase signaling pathways. Molecular pharmacology. 2007; 72:29–39. [PubMed: 17395690]
40. Yu L, McPhee CK, Zheng L, Mardones GA, Rong Y, Peng J, Mi N, Zhao Y, Liu Z, Wan F, et al. Termination of autophagy and reformation of lysosomes regulated by mTOR. Nature. 2010; 465:942–946. [PubMed: 20526321]
41. Kirkland RA, Adibhatla RM, Hatcher JF, Franklin JL. Loss of cardiolipin and mitochondria during programmed neuronal death: evidence of a role for lipid peroxidation and autophagy. Neuroscience. 2002; 115:587–602. [PubMed: 12421624]
42. Kissova I, Deffieu M, Samokhvalov V, Velours G, Bessoule JJ, Manon S, Camougrand N. Lipid oxidation and autophagy in yeast. Free Radic Biol Med. 2006; 41:1655–1661. [PubMed: 17145553]
43. Case BW, Ip MP, Padilla M, Kleinerman J. Asbestos effects on superoxide production: an in vitro study of hamster alveolar macrophages. Environmental research. 1986; 39(2):299–306. [PubMed: 3007104]
44. Roney PL, Holian A. Possible mechanism of chrysotile asbestos-stimulated superoxide anion production in guinea pig alveolar macrophages. Toxicology and applied pharmacology. 1989; 100(1):132–144. [PubMed: 2548304]
45. Bhattacharya K, Dopp E, Kakkar P, Jaffery FN, Schiffmann D, Jaurand MC, Rahman I, Rahman Q. Biomarkers in risk assessment of asbestos exposure. Mutation Research. 2005; 579(1):6–21. [PubMed: 16112146]
46. Gibson SB. A matter of balance between life and death: targeting reactive oxygen species (ROS)-induced autophagy for cancer therapy. Autophagy. 2010; 6:835–837. [PubMed: 20818163]
47. Shin S1, Jing K, Jeong S, Kim N, Song KS, Heo JY, Park JH, Seo KS, Han J, Park JI, Kweon GR, Park SK, Wu T, Hwang BD, Lim K. The omega-3 polyunsaturated fatty acid DHA induces simultaneous apoptosis and autophagy via mitochondrial ROS-mediated Akt-mTOR signaling in prostate cancer cells expressing mutant p53. BioMed research international. 2013; 2013:568671. [PubMed: 23841076]

48. Mossman BT, Lippmann M, Hesterberg TW, Kelsey KT, Barchowsky A, Bonner JC. Pulmonary endpoints (lung carcinomas and asbestosis) following inhalation exposure to asbestos. Journal of Toxicology and Environmental Health Part B. 2011; 14(1–4):76–121.

49. Wong C, Iskandar K, Yadav S, Hirpara J, Loh T, Pervaiz S. Simultaneous induction of non-canonical autophagy and apoptosis in cancer cells by ROS-dependent ERK and JNK activation. PLoS One. 2010; 5(4):e9996. [PubMed: 20368806]

50. Scherz-Shouval R, Weidberg H, Gonen C, Wilder S, Elazar Z, Oren M. p53-dependent regulation of autophagy protein LC3 supports cancer cell survival under prolonged starvation. Proc Natl Acad Sci USA. 2010; 107:18511–18516. [PubMed: 20937856]

51. Crighton D, Wilkinson S, O'Prey J, Syed N, Smith P, Harrison PR, Gasco M, Garrone O, Crook T, Ryan KM. DRAM, a p53-Induced Modulator of Autophagy, Is Critical for Apoptosis. Cell. 2006; 126:121–134. [PubMed: 16839881]

52. Chen SY, Chiu LY, Ma MC, Wang JS, Chien CL, Lin WW. zVAD-induced autophagic cell death requires c-Src-dependent ERK and JNK activation and reactive oxygen species generation. Autophagy. 2011; 7(2):217–228. [PubMed: 21127402]

53. Cagnol S, Chambard JC. ERK and cell death: Mechanisms of ERK-induced cell death–apoptosis, autophagy and senescence. FEBS Journal. 2009; 277(1):2–21. [PubMed: 19843174]

54. Barthwal MK, Sathyanarayana P, Kundu CN, Rana B, Pradeep A, Sharma C, Woodgett JR, Rana A. Negative regulation of mixed lineage kinase 3 by protein kinase B/Akt leads to cell survival. J Biol Chem. 2003; 278:3897–3902. [PubMed: 12458207]

55. Fey D, Croucher DR, Kolch W, Kholodenko BN. Crosstalk and signaling switches in mitogen-activated protein kinase cascades. Frontiers in physiology. 2012; 3:355–355. [PubMed: 23060802]

56. Roux PP, Blenis J. ERK and p38 MAPK-activated protein kinases: a family of protein kinases with diverse biological functions. Microbiology and molecular biology reviews. 2004; 68(2):320–344. [PubMed: 15187187]

57. Amaravadi RK, Yu D, Lum JJ, Bui T, Christophorou MA, Evan GI, Thomas-Tikhonenko A, Thompson CB. Autophagy inhibition enhances therapy-induced apoptosis in a Myc-induced model of lymphoma. Journal of Clinical Investigation. 2007; 117(2):326. [PubMed: 17235397]

58. Soberanes S, Panduri V, Mutlu GM, Ghio A, Bundinger GS, Kamp DW. p53 Mediates Particulate Matter–induced Alveolar Epithelial Cell Mitochondria-regulated Apoptosis. American journal of respiratory and critical care medicine. 2006; 174(11):1229. [PubMed: 16946128]

59. Matoba S, Kang JG, Patino WD, Wragg A, Boehm M, Gavrilova O, Hurley PJ, Bunz F, Hwang PM. p53 regulates mitochondrial respiration. Science. 2006; 312(5780):1650–1653. [PubMed: 16728594]

Appendix A. Supplemental Data

Supplemental Data include five figures.

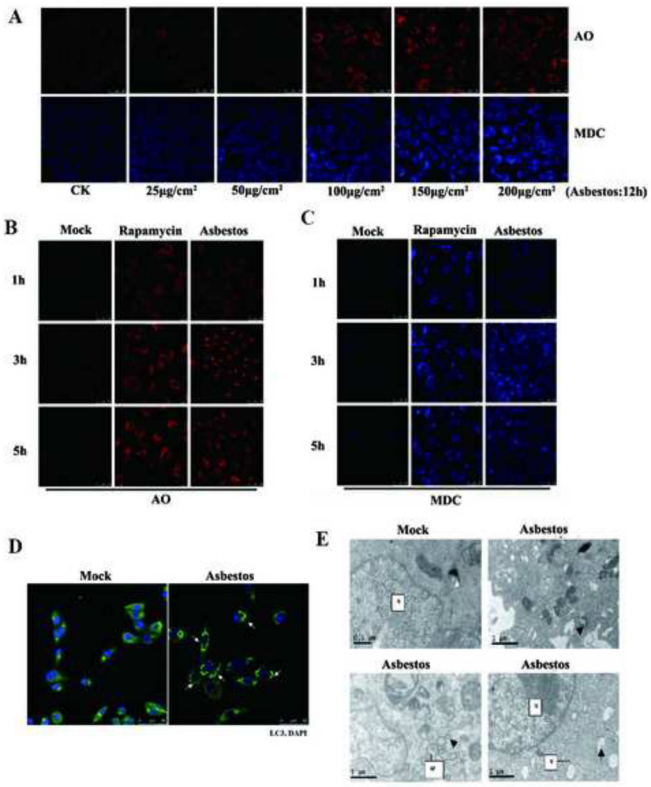

Fig. 1. Autophagy is characterized by the formation and promotion of AVOs and autophagosomes

(A–C) A549 cells were treated with different concentrations of chrysotile asbestos or with 100 μg/cm^2 chrysotile asbestos at different time duration with rapamycin as positive control. The cells were stained with 1 mg/ml acridine orange or 50 mM MDC for 15 min. After incubation, cells were immediately analyzed by a confocal microscope. Red: acidic vesicular organelle. Blue: MDC. (D) Confocal images of LC3 expression in chrysotile asbestos-treated A549 cells. Arrows indicate LC3 puncta (green), DAPI (blue); bar, 50 μm. (E) EM images of A549 cells treated with vehicle (PBS) or chrysotile asbestos(100μg/cm^2). Arrows indicate autophagosomes. Scale bar, 1 μm.

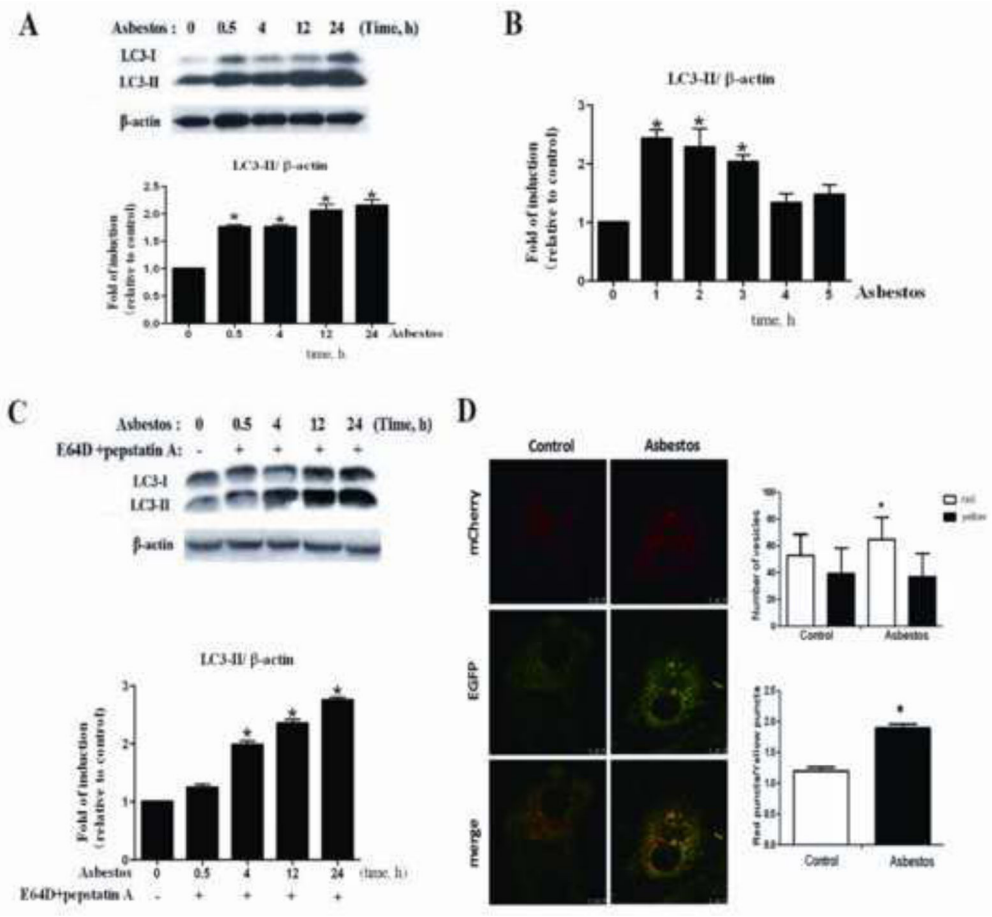

Fig. 2. Autophagy was induced in A549 cells upon exposure to chrysotile asbestos

(A) Western blot analysis of LC3-I and LC3-II expression in A549 cells treated with chrysotile asbestos(100 μg/cm^2) for the indicated time duration (0–5h). Band intensity was calculated using Image J software and the ratio of LC3-II/β-actin was determined. The protein expression level of control (0 h) group was arbitrarily set to 1 in each blot, and the signals from other experimental conditions in the same blot were normalized to the control to indicate their protein expression level. (B) Quantitative reverse transcription-PCR analysis of LC3-II. A549 cells were treated with chrysotile asbestos for the indicated time. Each bar represents the mean ± SD derived from three independent assays in triplicate, **P*<0.05. (C) Western blot revealed an increase in LC3-II in the presence of the lysosomal inhibitors E64d (10 μg/ml) + Pepstatin A (10 μg/ml) after exposure to chrysotile asbestos. The intensity of these protein signals obtained was quantified using Image J software from three replicate experiments. (D) A549 cells were transfected with mCherry-EGFP-LC3-II and treated with chrysotile asbestos. Cells with autolysosomes (more than five autolysosomes in a cell) were sampled from a pool of at least 10 images. The difference of autophagic flux results between groups expressing mRFP-EGFP-LC3 was evaluated for statistical significance using Student's t-test. **P*<0.05. Pearson's correlation coefficient was used as a measure of colocalization of RFP signals with GFP signals. Correlation plot is corresponding to the left figure. The mean correlation coefficient value ± SEM of at least five cells is shown on the plots. Scale bar: 50 μm.

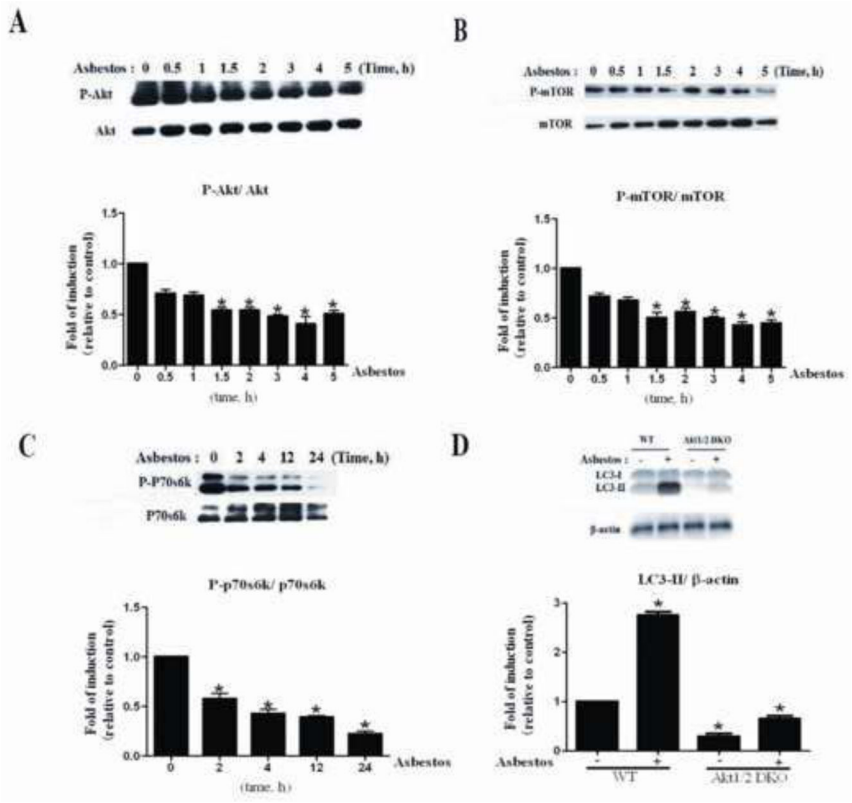

Fig. 3. Chrysotile asbestos treatment induced autophagy in A549 cells and MEFs via the PI3K/AKT/mTOR pathway

A549 cells were treated with chrysotile asbestos for the indicated time (0–24 h). The expression levels of the indicated proteins were analyzed by immunoblotting. (A–C) Western blot assays were used to examine the total and phosphorylated protein levels of AKT, mTOR, and P70S6K. Densitometry signals were normalized to those of total protein, then normalized to those of untreated A549 cells (100%). (D) Western blot of LC3 in WT and AKT (DKO) MEF cells. The ratio of LC3II/β-actin was determined. The intensity of these protein signals obtained was quantified using Image J software from three replicate experiments.

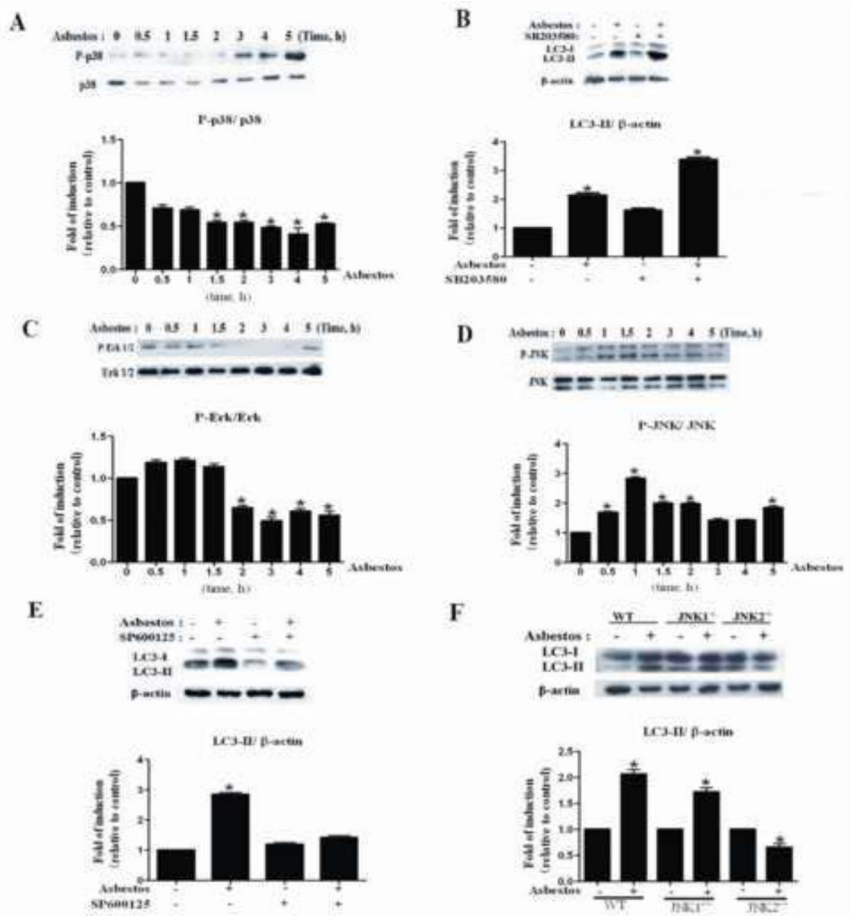

Fig. 4. JNK signaling pathway is required for chrysotile asbestos-induced autophagy

(A, C, D) Western blot assays were used to examine the total and phosphorylated protein levels of p38 MAPK, ERK1/2 and JNK. (B, E) The effects of inhibitors on the expression of LC3-II induced by chrysotile asbestos in A549 cells. p38 MAPK inhibitor SB203580 (10 μM) and JNK inhibitor SP600125 were pretreated 1h before chrysotile asbestos treatment. In the absence or presence of chrysotile asbestos, A549 cells were pretreated with the inhibitors for 5h. The ratio of LC3-II/β-actin was determined. (F) The effect of chrysotile asbestos on the expression of LC3II in the WT and JNK1$^{-/-}$ and JNK2$^{-/-}$ MEF cells. The ratio of LC3-II/β-actin was determined. The intensity of these protein signals obtained was quantified using Image J software from three replicate experiments.

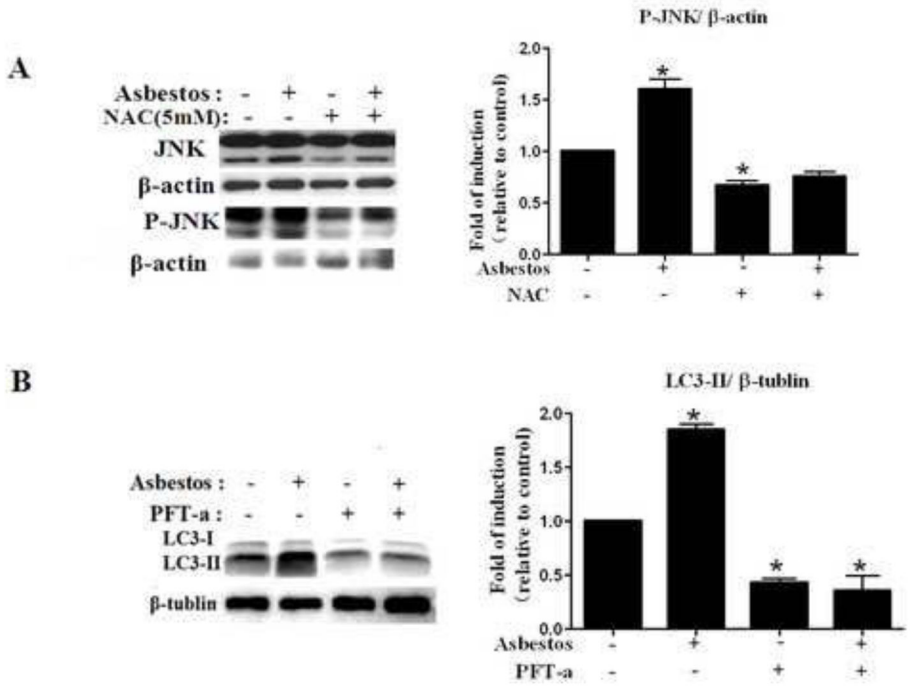

Fig. 5. ROS and p53 are involved in chrysotile asbestos-induced autophagy

(A) Western blot of p-JNK in control cells, cells treated with 100 μg/cm^2 chrysotile asbestos or 100 μg/cm^2 chrysotile asbestos plus 5 mM NAC for 24 h. (B) Western blot of LC3 in control cells, cells treated with 100 μg/cm^2 chrysotile asbestos or 100μg/cm^2 chrysotile plus 30 μM pifithrin-α for 5 h. The ratio of LC3-II/β-tublin was determined. The intensity of these protein signals obtained was quantified using Image J software from three replicate experiments.

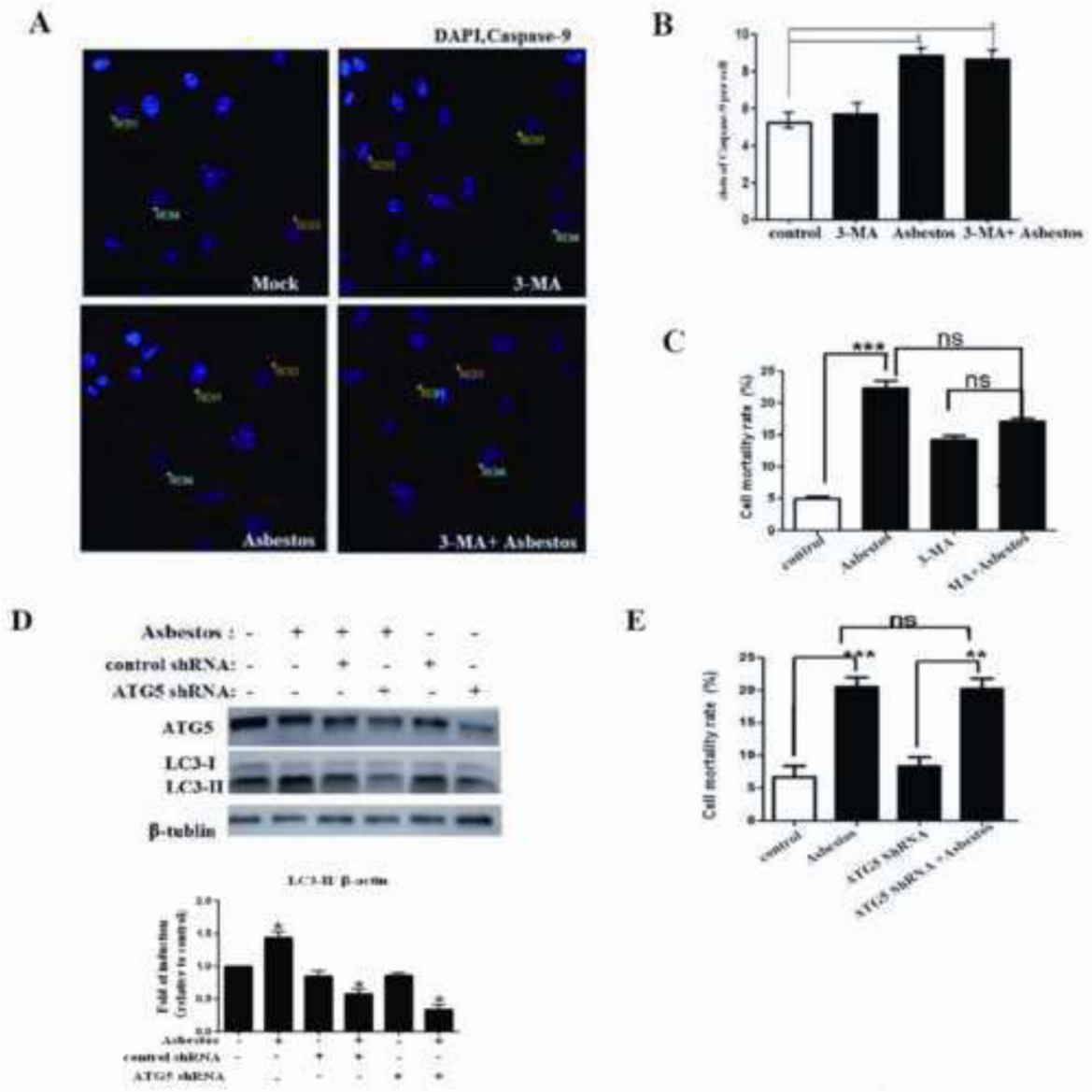

Fig. 6. Inhibition of autophagy is not responsible for chrysotile asbestos-induced cell death

(A) The fluorescent images of A549 cells labeled with caspase-9(red) and DAPI (blue). Scale bar: 20 μm. The cells were incubated with 100 μg/cm^2 chrysotile asbestos for 24 h, in the presence or absence of 10 mM 3-MA. (B) Caspase-9 dot formation was observed and quantified as shown in Fig. 6A, n=12, **P*<0.05. (C, E) Effect of 3-MA and ATG5 siRNA on the survival of chrysotile asbestos-treated A549 cells as determined by Trypan blue dye exclusion assay. Data are mean ± SEM (N=3). *indicates significant difference in values compared with control (*P*<0.05) as measured by one-way ANOVA. (D) Western blot of ATG5 and LC3. A549 cells were transiently transfected with negative control siRNA and ATG5 siRNA. The transfected cells were then treated with 100μg/cm^2 chrysotile asbestos for 24 h. The ratio of LC3-II/β-tublin was determined.